In Silico Pharmacophore Model for Tabun-Inhibited Acetylcholinesterase Reactivators: A Study of Their Stereoelectronic Properties

Apurba K. Bhattacharjee,*[,†] Kamil Kuča,[‡,§] Kamil Musilek,[‡] and Richard K. Gordon[†]

Department of Regulated Laboratories, Division of Regulated Activities, Walter Reed Army Institute of Research, 503 Robert Grant Avenue, Silver Spring, Maryland 20910, and Center for Advanced Studies and Department of Toxicology, Faculty of Military Health Sciences, Třebešská 1575, Hradec Králové, Czech Republic

Received June 9, 2009

Organophosphorus (OP) nerve agents that inhibit acetylcholinesterase (AChE; EC 3.1.1.7) function in the nervous system, causing acute intoxication. If untreated, death can result. Inhibited AChE can be reactivated by oximes, antidotes for OP exposure. However, OP intoxication caused by the nerve agent tabun (GA) is particularly resistant to oximes, which poorly reactivate GA-inhibited AChE. In an attempt to develop a rational strategy for the discovery and design of novel reactivators with lower toxicity and increased efficacy in reactivating GA-inhibited AChE, we developed the first in silico pharmacophore model for binding affinity of GA-inhibited AChE from a set of 11 oximes. Oximes were analyzed for stereoelectronic profiles and three-dimensional quantitative structure−activity relationship pharmacophores using ab initio quantum chemical and pharmacophore generation methods. Quantum chemical methods were sequentially used from semiempirical AM1 to hierarchical ab initio calculations to determine the stereoelectronic properties of nine oximes exhibiting affinity for binding to GA-inhibited AChE in vivo. The calculated stereoelectronic properties led us to develop the in silico pharmacophore model using CATALYST methodology. Specific stereoelectronic profiles including the distance between bisquarternary nitrogen atoms of the pyridinium ring in the oximes, hydrophilicity, surface area, nucleophilicity of the oxime oxygen, and location of the molecular orbitals on the isosurfaces have important roles for potencies for reactivating GA-inhibited AChE. The in silico pharmacophore model of oxime affinity for binding to GA-inhibited AChE was found to require a hydrogen bond acceptor, a hydrogen bond donor at the two terminal regions, and an aromatic ring in the central region of the oximes. The model was found to be well-correlated ($R = 0.9$) with experimental oxime affinity for binding to GA-inhibited AChE. Additional stereoelectronic features relating activity with the location of molecular orbitals and weak electrostatic potential field over the aromatic rings were found to be consistent with the pharmacophore model. These results provided the first predictive pharmacophore model of oxime affinity for binding toward GA-inhibited AChE. The model may be useful for virtual screening of compound libraries to discover and/or custom synthesize more efficacious and less toxic reactivators that may be useful for GA intoxication.

Introduction

Organophosphorus (OP) compounds, such as tabun (GA), soman, sarin, or cyclosarin, and pesticides [paraoxon, chlorpyrifos, and tetraethyl pyrophosphate (TEPP)] represent an extremely toxic group of compounds (*1*). Nerve agents such as GA are considered potential warfare threats due to their high intrinsic toxicity. OPs have documented uses in war, for example, the use of VX used in the Iran−Iraq war, and in civilian attacks by terrorists, for example, the use of sarin in a Tokyo subway (*2*). The acute toxicity of OP compounds in mammals is due to inhibition of the enzyme acetylcholinesterase (AChE; EC 3.1.1.7) and subsequent accumulation of the neurotransmitter acetylcholine (ACh) in synapses of the central and peripheral nervous systems, resulting in overstimulation of postsynaptic cholinergic receptors (*1*). Exposure to OP compounds causes a progression of toxic signs including hypersecretions, fasciculation, tremors, convulsions, coma, respiratory distress, and, eventually, death. AChE is a serine hydrolase responsible for hydrolyzing (removing) the neurotransmitter ACh in humans and animals. The enzyme has a catalytic triad consisting of Ser203, His447, and Glu334 at the active site in a narrow deep gorge (∼20 Å), the lining of which contains mostly aromatic residues that form a narrow entrance to the catalytic Ser203 (*3*). A peripheral anionic site (PAS) comprising another set of aromatic residues Tyr72, Tyr124, Trp286, and Tyr341 and acidic Asp74 (*4*) is located at the rim of this gorge and provides a binding site for allosteric modulators and inhibitors. AChE is inhibited by OP agents through a phosphorus group that is conjugated to the catalytic serine residue at the active site (*3*).

The conjugate of the inhibited AChE may either undergo a process known as "aging" via an elimination reaction involving dealkylation/deamidation, which is irreversible, or, prior to the "aging", undergo reactivation by nucleophiles such as oximes (*5*, *6*). The current standard treatment for OP poisoning includes a muscarinic receptor antagonist, atropine, to block the overstimulation of cholinergic receptors by ACh accumulation and an oxime to reactivate OP-inhibited AChE (*1*). Pralidoxime (2-PAM), obidoxime, and HI-6 are the most commonly used

* To whom correspondence should be addressed. Tel: 301-319-9043. Fax: 301-319-9070. E-mail: Apurba.Bhattacharjee@amedd.army.mil.
† Walter Reed Army Institute of Research.
‡ Center for Advanced Studies, Faculty of Military Health Sciences.
§ Department of Toxicology, Faculty of Military Health Sciences.

10.1021/tx900192u

Report Documentation Page

Form Approved
OMB No. 0704-0188

1. REPORT DATE	2. REPORT TYPE	3. DATES COVERED
09 JUN 2009		**00-00-2009 to 00-00-2009**

4. TITLE AND SUBTITLE	5a. CONTRACT NUMBER
In Silico Pharmacophore Model for Tabun-Inhibites Acetylcholinesterase Reactivators: A study of their Sterelectronic Properties	5b. GRANT NUMBER
	5c. PROGRAM ELEMENT NUMBER
6. AUTHOR(S)	5d. PROJECT NUMBER
	5e. TASK NUMBER
	5f. WORK UNIT NUMBER
7. PERFORMING ORGANIZATION NAME(S) AND ADDRESS(ES) **Department of Regulated Laboratories, Division of Regulated Activities,Walter Reed Army Institue of Research,503 Robert Grant Avenue,Silver Spring,MD,20910**	8. PERFORMING ORGANIZATION REPORT NUMBER
9. SPONSORING/MONITORING AGENCY NAME(S) AND ADDRESS(ES)	10. SPONSOR/MONITOR'S ACRONYM(S)
	11. SPONSOR/MONITOR'S REPORT NUMBER(S)

12. DISTRIBUTION/AVAILABILITY STATEMENT
Approved for public release; distribution unlimited

13. SUPPLEMENTARY NOTES

14. ABSTRACT

15. SUBJECT TERMS

16. SECURITY CLASSIFICATION OF:			17. LIMITATION OF ABSTRACT	18. NUMBER OF PAGES	19a. NAME OF RESPONSIBLE PERSON
a. REPORT	b. ABSTRACT	c. THIS PAGE			
unclassified	**unclassified**	**unclassified**	**Public Release**	**11**	

Chart 1. Structures of the Oximes Used for Developing the Pharmacophore Model

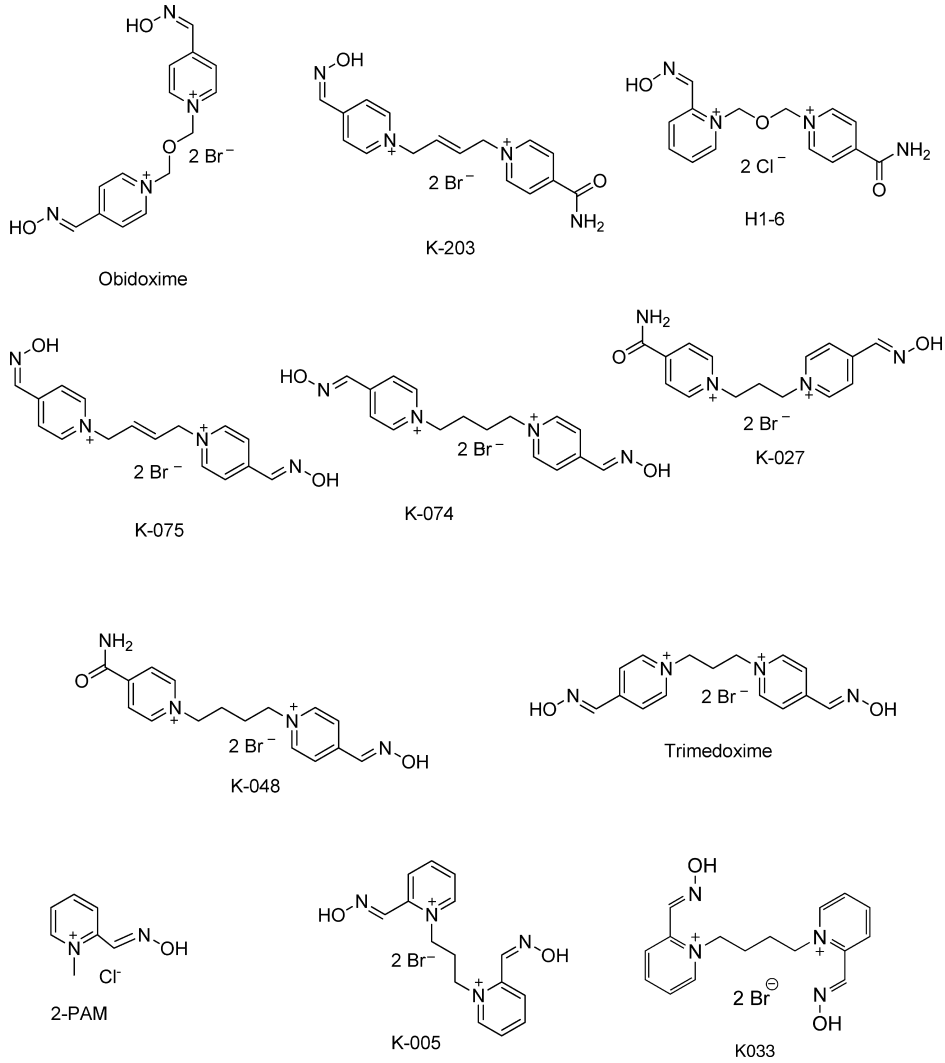

oximes for the treatment of OP exposure. These compounds, containing a quaternary nitrogen that promotes binding in the catalytic site of the AChE, are now considered the standard treatments for OP exposure (*1*). The mechanism of reactivation requires a nucleophilic group from the oximes, which cleaves the OP-inhibited moiety of AChE and thus restores its functional ability (*7*). However, the nerve agent GA is found to be resistant to the common oximes (*8a, 8b*). In fact, none of the above oximes can be regarded as a broad spectrum antidote to all nerve agents. For example, VX-inhibited AChE can be reactivated efficiently by the oxime HI-6, whereas HI-6 is far less efficacious for GA-inhibited AChE (*9*). From structure−activity relationship (SAR) studies, Musilek et al. (*10*) reported that steric hindrance induced by GA-inhibited AChE led to partial closing of the enzyme's active site so that few bipyridinum oximes can enter the active site to reactivate GA-inhibited AChE. It was further hypothesized that the existence of a lone pair of electrons located on an amidic group of GA makes the nucleophilic attack by oximes ineffective (*11*). Thus, treatment of GA poisoning with oximes is much more difficult and challenging, suggesting the need for new oximes to reactivate GA-inhibited AChE.

We present here the first in silico pharmacophore model of oxime affinity for GA-inhibited AChE derived from theoretical stereoelectronic and three-dimensional (3D) quantitative structure−activity relationship (QSAR) pharmacophore analyses. Because the efficacy of an oxime to reactivate AChE depends on its affinity for the nerve agent inhibited enzyme, it is an important parameter for overall reactivating efficacy because reactivation is critically related to binding of the oxime to the inhibited enzyme followed by breakdown of the inhibited complex (*12*). The model developed in this paper reflects the affinity of an oxime for the GA-inhibited enzyme. Our pharmacophore is based on recently reported binding affinity (*13, 14*) of 11 oximes (Chart 1) for GA-inhibited AChE. The oximes were seven K-oximes including the potential candidate for treatment of GA intoxication in vivo: (*E*)-1-(4-carbamoylpyridinium)-4-(4 hydroxyiminomethylpyridinium)-but-2-ene dibromide (K203), obidoxime, HI-6, trimedoxime, and 2-PAM. We performed QSAR studies with nine oximes ranging from AM1 (Austin Model 1) semiempirical to hierarchical ab initio quantum chemical calculations and pharmacophore generation with 11 oximes to assess the role of calculated properties toward binding affinity of the oximes for GA-inhibited AChE.

More recently, quantum chemical descriptors have been used in QSAR studies because of the large well-defined physical information content encoded in many of these theoretical descriptors (*15*). The ability of a bioactive molecule to interact with the recognition sites in receptors or active sites of enzymes results from a combination of steric and electronic properties. Therefore, the study of stereoelectronic properties of these molecules can provide valuable information not only to better understand the mechanism of action but also to view the intrinsic "interaction pharmacophore" profile to aid in the design of more

Chart 2. Structures of the Oximes Used for Testing the Pharmacophore Model

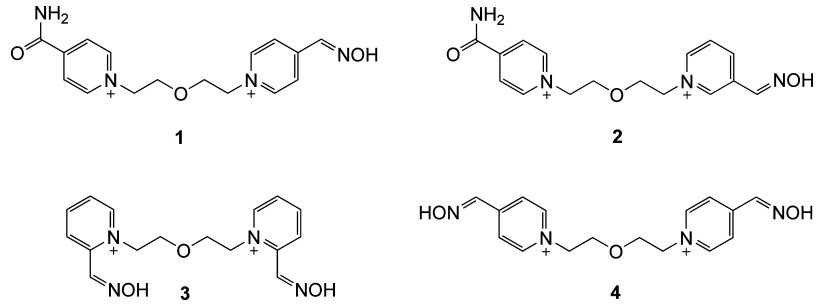

efficient compounds. Thus, study of the stereoelectronic properties of a series of bispyridinium oximes that reactivate GA-inhibited AChE could provide insight for designing more efficacious oximes (*5, 6*). Quantum chemical methods accurately estimate stereoelectronic properties of molecules and "interaction-pharmacophores" (*16, 17*).

An in silico pharmacophore, a "three dimensional pharmacophore", may be perceived as a geometric distribution of chemical features such as a hydrogen bond acceptor, hydrogen bond donor, aliphatic and aromatic hydrophobic functions, ring aromatic hydrophobicity, and other parameters describing the specific biological activity in a 3D space of a drug (*18*). Pharmacophores may be derived in several ways, for example, by analogy to a natural substrate or known ligand, by inference from a series of dissimilar active analogs, or by direct analysis of the structure of a target protein (*18*). A pharmacophore can be used in two ways to identify new compounds that share its features and may thus exhibit a desired biologic response. In the first approach, de novo design can be performed that links the disjointed parts of the pharmacophore together with fragments to generate hypothetical structures that are chemically reasonable but completely novel. The second approach uses the pharmacophore model to search 3D compound databases. A key advantage of 3D database searching over de novo design is that it identifies existing compounds that are readily available and have known synthetic procedures. In the later case, pharmacophores generated by multiple conformations from a set of structurally diverse molecules enable rapid screening of virtual molecules/libraries to identify potent and nonpotent ligands (*19, 20*).

Materials and Methods

Procedure Followed for Quantum Chemical Calculations. Conformation search calculations were performed using the "systematic search" technique via single-point AM1 method in SPARTAN (*21*) to generate different conformers for each of the molecules. The minimum energy conformer with the highest abundance (a Boltzman population density greater than 70.0%) was chosen for full geometry optimization using the AM1 algorithm (*22*) followed by reoptimizations at the ab initio quantum chemical level using hierarchical basis sets of the Gaussian98 package (*23*). AM1 is a semiempirical quantum chemistry method. It is based on the Hartree−Fock formalism but, like all other semiempirical methods, makes approximations and obtains some parameters from empirical data. Two main approximations make the method computationally time effective. First, the size problem of a molecule (number of atoms) is reduced by restricting treatment to valence electrons only. Second, the basis set, molecular orbitals expressed as linear combinations of a finite set of prescribed functions, is restricted to a minimal representation. The central approximation, in terms of reducing overall computation, is to insist that atomic orbitals residing on different atomic centers do not overlap. These considerations are important when treating large molecules where the full Hartree−Fock method without the approximations is too time-consuming computationally (*22*). Geometry optimizations were carried out sequentially at increasing levels of theory or basis sets as inputs starting from the AM1 optimized geometry on the singlet states of neutral molecules. Restricted Hartree−Fock (RHF) calculations at the 6-31G** polarized (d,p) basis set level were found to be adequate for this size of molecules since substantially higher basis sets were found to produce similar trends (*24*). The computations were carried out on a Silicon Graphics Octane workstation. To simulate physiological conditions, complete geometry optimization of the molecules was performed in the presence of an aqueous environment using the AM1aq method developed by Dixon et al. (*25*) in SPARTAN and, subsequently, single point calculations using the ab initio polarizable continuum model (SCRF=PCM) (*26*). Molecular electronic properties such as the molecular orbital energies, electrostatic potentials, octanol−water partition coefficients (log *P*), and other structural parameters were calculated on the optimized geometry of each of the molecules as implemented in the above software.

Molecular electrostatic potential (MEP) maps and molecular orbital isosurfaces were generated and sampled over the entire accessible surface of a molecule (corresponding roughly to a van der Waals contact surface) using the graphics of SPARTAN (*21*). The MEP maps provide a measure of charge distribution from the point of view of an approaching reagent. The orbital isosurfaces locate positions and magnitudes of the orbitals where it is available outside the normal steric volume of the molecule for interactions with the complementary orbitals.

Procedure for Generation of 3D Pharmacophore Model. A 3D pharmacophore model was developed using the CATALYST 4.10 methodology (*27*). Although the recommended procedure for a training set in CATALYST is to use 15−20 compounds with experimental activity data, we had to use the present training set of 11 compounds because these were the only oximes found in the published literature that were tested under identical laboratory conditions of physiological pH, carried out at room temperature, had sufficient diversity data for affinity toward the GA-inhibited AChE, reactivation efficacy data in terms kinetic parameters, and were reported to have over 95% confidence limit on the experiments (*13, 14*). However, we tested the predictive ability of the model using an additional publication (*28*) providing experimental dissociation constants, K_R, values for three of the four reported different K-oximes: 1-(4-hydroxyiminomethylpyridinium)-5-(4-carbamoylpyridinium)-3-oxa-pentane, **1**; 1-(3-hydroxyiminomethylpyridinium)-5-(4-carbamoylpyridinium)-3-oxa-pentane, **2**; 1,5-bis-(2-hydroxyiminomethylpyridinium)-3-oxa-pentane, **3**; 1,5-bis-(4-hydroxyiminomethylpyridinium)-3-oxa-pentane, **4**; (Chart 2), and HI-6, obtained under the same experimental conditions. None of these four compounds were considered for generating the training set.

CATALYST is an integrated commercially available software package (*27*) that generates pharmacophores, commonly referred to as hypotheses in the CATALYST terminology. It enables the use of structure and activity data for a set of lead compounds to create a hypothesis, thus characterizing the activity of the lead set. The software is based on the HypoGen algorithm that allows identification of hypotheses that are common to the "active" molecules in the training set but at the same time not present in

the "inactives" (*18*). The algorithm treats molecular structures as templates comprised of chemical functions localized in space that will bind effectively with complementary functions on the respective binding proteins. The most relevant biological features are extracted from a small set of compounds that cover a broad range of activity. It enables the use of structure and activity data for a set of lead compounds to generate a pharmacophore characterizing the activity of the lead set. Conformational models of molecules were generated by creating a training set of all of the oximes that emphasize representative coverage within a range of the permissible Boltzman population with significant abundance (within10.0 kcal/mol) of the calculated global minimum. We selected this conformational model for pharmacophore generation within CATALYST, which aims to identify the best 3D arrangement of chemical features such as hydrophobic regions, hydrogen bond donor, hydrogen bond acceptor, and positively and/or negatively ionizable sites distributed over a 3D space explaining the activity variations among the training set. The hydrogen-bonding features are vectors, whereas all other functions are points.

Pharmacophore generation for the oximes based on experimentally obtained data (*13, 14*) from GA-inhibited AChE was carried out by setting the default parameters in the automatic generation procedure in CATALYST such as function weight, 0.302; mapping coefficient, 0; resolution, 287 pm; and activity uncertainty, 3. An uncertainty "Δ" in the CATALYST paradigm indicates an activity value lying somewhere in the interval from "activity divided by Δ" to "activity multiplied by Δ". Hypotheses approximating the pharmacophore of the oximes were described as a set of aromatic hydrophobic, hydrogen bond acceptor, hydrogen bond acceptor lipid type, hydrogen bond donor, and positively and negatively ionizable sites distributed over a 3D space. The statistical relevance of various generated hypotheses was assessed on the basis of the cost relative to the null hypothesis and the correlation coefficients. The hypotheses were then used to estimate the activities of each of the 11 oximes. These activities are derived from the best conformation generation mode of the conformers displaying the smallest root mean square (rms) deviations when projected onto the hypothesis. HypoGen considers a pharmacophore that contain features with equal weights and tolerances. Each feature (e.g., hydrogen bond acceptor, hydrogen bond donor, hydrophobic, positive ionizable group, etc.) contributes equally to estimate the activity. Similarly, each chemical feature in the HypoGen pharmacophore requires a match to a corresponding ligand atom to be within the same distance (tolerance) (*27*). Thus, two parameters, fit score and conformational energy costs, are crucial for the estimation of predicted activity of the compounds. This method has been documented to perform better than a structure-based pharmacophore generation (*29*). To avoid chance correlation, statistical relevance of the obtained pharmacophore was assessed on the basis of cost relative to the null hypothesis (see the *.log file in the Supporting Information) and the correlation coefficient with CatScrambled confidence level of the pharmacophore (*27*). CatScrambled performs Fischer randomization calculations on the pharmacophore models as implemented in the CATALYST (*27*). Using this technique, several models can be generated from the training set, and the statistical significance of each model can be calculated and assessed for their respective total cost requirements and confidence level of a particular pharmacophore. The details of the results of randomization calculations are presented in the Results and Discussion.

Procedure for General Preparation of These Compounds. Candidates for the reactivation of GA-inhibited AChE generally require two oxime groups (quaternary nitrogen atoms and bis-oximes) in comparison to one quaternary nitrogen for other organophosphates. In addition, more potent reactivators were found to require at least one oxime group at the 4-position of the pyridinium ring and a 3−4 member linker between the two pyridinium rings. The basic structure for synthesis of a GA-inhibited AChE reactivator is shown in the sketch below:

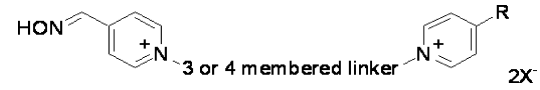

Detailed procedures for synthesis of these compounds have been reported (*13, 30, 31*).

Results and Discussion

Initially, we performed stereoelectronic property calculations using semiempirical AM1 and hierarchical ab initio quantum chemical methods on the nine oxime reactivators (*13*) of GA-inhibited AChE (Chart 1), which yielded a more accurate "interaction pharmacophore" profiles for the oximes. We carried out conformational analysis and Boltzmann abundance calculations on the oximes and fully optimized each of the most abundant minimum energy conformer using the AM1 method (*21, 22*). AM1 optimized structures were further optimized using hierarchical RHF quantum chemical calculations starting from the minimum basis set of RHF/3-21G (*23*). For this set of oximes, the optimal basis set was found to be RHF/6-31G** doubly polarized (d, p) basis since the higher basis sets were found to produce similar trends (*24*). Only results from the RHF/6-31G** level of stereoelectronic property calculations are presented here, and detailed analysis and discussions are described below.

Stereoelectronic Characteristics. Calculated stereoelectronic properties and profiles of the nine oxime reactivators along with the reported (*13*) affinity for GA-inhibited AChE are presented in Tables 1 and 2. The optimized geometry of the nine oximes is shown in Figure 1, and the stereoelectronic profiles are presented in Figures 2S−6S of the Supporting Information. A comparison of the optimized geometry (Figure 1) of the reactivators and their affinity for GA-inhibited AChE indicates that obidoxime and trimedoxime have some significant differences despite certain apparent similarities in shape and geometry in comparison to other oximes in the present study. These two oximes are the only non K-oxime compounds having two terminal oximes groups with a 3-atom spacer between the two positively charged nitrogen atoms of the two pyridinium rings. The only difference is the ether oxygen atom (−O−) between the rings in obidoxime in comparison to a methylene ($-CH_2-$) group in trimedoxime. MEP surface profiles (Figure 2S of the Supporting Information) as well as the highest occupied molecular orbitals (HOMO) and lowest unoccupied molecular orbitals (LUMO) and surface profiles of the two compounds appear similar (Figures 3S−6S of the Supporting Information). However, the magnitudes of MEPs, HOMO and LUMO energies, total reactivity indexes, aqueous stabilization energy, and calculated octanol/water partition coefficient (log *P*) between the compounds change only marginally. Despite some similar stereoelectronic attributes between obidoxime and trimedoxime, obidoxime has a much greater affinity for GA-inhibited AChE than trimedoxime (Tables 1 and 2), demonstrating the importance of the ether linker in obidoxime. Thus, a specific electronic contribution likely plays an important role in increasing its binding affinity as compared to trimedoxime against GA-inhibited AChE (*6*).

Because oximes exhibit toxicity at high doses, more potent reactivators with reduced toxicity are needed (*32*). Musilek et al. (*13*) reported five K-oximes, three of which (K-203, K-027, and K-048) have one oxime moiety replaced by a carbamoyl group combined with different linkers between the pyridinium moieties. Of these five K-oximes, K-203 is slightly less toxic than K-074 and K-075, whereas K-027 and K-048 were reported to be least toxic (*12*) (Chart 1). However, the trend from our in silico rat oral LD_{50} assessment (Table 2) using TOPKAT (*33*) shows the following decreasing order on the eight compounds:

Table 1. Calculated Stereoelectronic Properties (ab Initio RHF/6-31G) and Affinity for GA-Inhibited AChE**

compound	distance (Å) N^+-N^+	density	molecular volume (A^3)	surface area (A^2)	affinity for inhibited enzyme (μM) (experimental) (*13*)
obidoxime	4.58	1.0	286.5	320.0	3.0
K-203	5.76	0.96	308.4	336.6	6.0
HI-6	4.23	1.01	284.2	309.1	6.0
K-075	5.87	0.96	310.3	343.5	19.0
K-074	6.31	0.95	314.4	348.3	29.0
K-027	4.99	0.97	294.9	325.9	54.0
K-048	6.04	0.95	313.3	345.8	93.0
trimedoxime	5.0	0.96	296.1	328.3	460.0
2-PAM	2.94	0.94	145.0	167.0	575.0

Table 2. Calculated Stereoelectronic Properties (ab Initio RHF/6-31G and Empirical Methods) and Affinity for GA-Inhibited AChE**

compound	aqueous stabilization (kcal/mol)	log P	MEP (kcal/mol) low	MEP (kcal/mol) high	electrostatic charge separation (kcal/mol)	HOMO (eV)	LUMO (eV)	HOMO−LUMO energy gaps (eV)	calculated rat oral LD_{50} (mg/kg)	affinity for inhibited enzyme (experimental) (μM) (*13*)
obidoxime	148.5	0.37	68.1	189.3	121.2	−15.6	−5.3	10.3	1100	3.0
K-203	150.3	−0.29	46.1	182.9	136.8	−15.6	−5.0	10.6	502.7	6.0
HI-6	151.5	0.9	69.3	202.3	133.0	−16.1	−5.5	10.6	807.4	6.0
K-075	142.5	0.48	64.0	175.1	111.1	−15.3	−4.8	10.5	643.3	19.0
K-074	141.3	0.53	61.8	172.8	111.0	−15.2	−4.6	10.5	424.5	29.0
K-027	154.6	−0.52	48.6	188.0	139.4	−15.5	−5.2	10.3	568.4	54.0
K-048	148.6	−0.24	44.7	181.9	137.2	−15.3	−4.8	10.4	321.4	93.0
trimedoxime	148.8	0.25	65.7	182.7	117.0	−15.4	−5.0	10.4	722.8	460.0
2-PAM	46.9	1.41	40.2	138.5	98.3	−13.8	−2.9	10.8	477.4	575.0

K-048 < K-074 < K-203 < K027 < K-075 < trimedoxime < HI-6 < obidoxime, indicating higher toxicity as a whole for the K-oximes as compared to the currently available oximes (Table 2). Note that the calculated in silico toxicity values were based on rat oral doses, whereas Kassa et al. (*31*) reported LD_{50} values for the oximes following i.m. administrations in mice. Calculated stereoelectronic profiles of the nine oximes (Figure 1 and Figures 2S−6S of the Supporting Information) indicated large differences. The oximes HI-6, K-203, K-027, and K-048, which have one of the oxime moieties replaced with a carbamoyl group at the terminal end of the molecule (Chart 1), were prepared to reduce toxicity and, similar to HI-6, to improve efficacy. In silico rat oral LD_{50} assessment of these compounds indicated higher toxicity of these three K-oximes as compared to HI-6. HI-6 is currently considered the most broad spectrum reactivator for nerve agent intoxication, although not sufficiently efficacious to reactivate GA-inhibited AChE (*34*).

The nature of HI-6 was further explored; the optimized geometry of HI-6 is different from the other eight oximes (Figure 1). It exhibits the most bent geometry among all of the eight bipyridinium oximes in the set with the ether linker between the two pyridinium moieties (N^+-N^+ distance 4.23 A), which indicates a likely formation of an intramolecular hydrogen bonding between the hydroxyl hydrogen atom of the oxime and

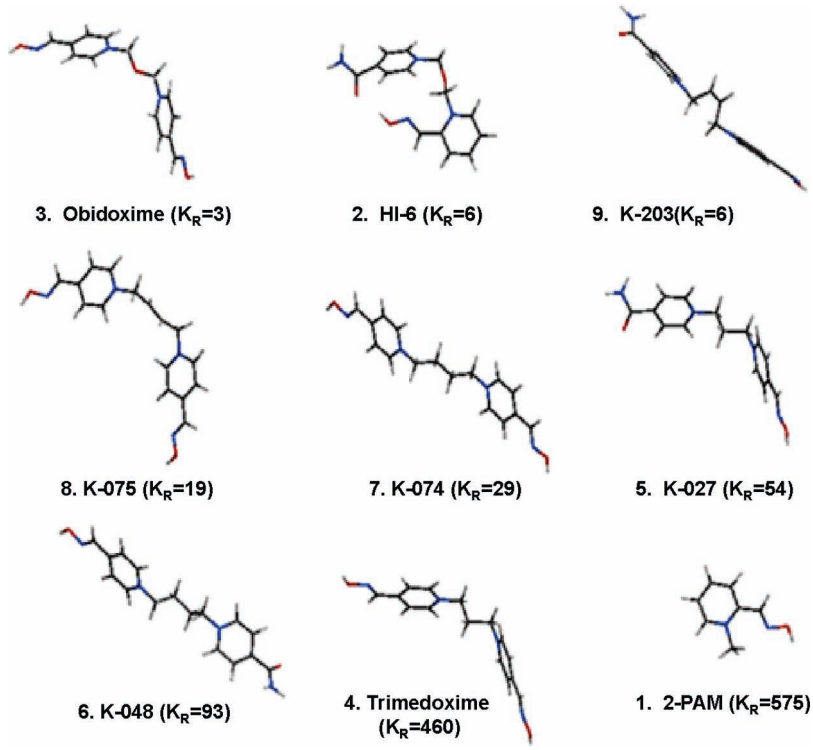

Figure 1. Optimized structures of nine oximes (shown in order of decreasing affinity for GA-inhibited AChE at the RHF/6-31G** level of ab initio QM theory).

the carbonyl oxygen of the carbamoyl group (approximate distance, 2.03 Å). Consequently, HI-6 geometry generated a lower surface area and volume with higher molecular density as compared to all of the other oximes (Table 1) except for 2-PAM. This geometry also resulted in HI-6 differing from the other oximes in surface MEP and HOMO and LUMO energy values (Table 2) and isosurfaces (Figures 2S, 4S, and 6S of the Supporting Information). The lowest and the highest MEP values, particularly the most positive potentials (a measure of intrinsic electrophilicity), the HOMO and LUMO energies (Table 2), and the HOMO and LUMO orbitals (Figures 2S, 3S, and 5S of the Supporting Information) of HI-6 differ significantly from the rest of the oximes. HI-6's stereoelectronic differences likely contribute toward its stronger binding affinity and weaker reactivation efficacy for GA-inhibited AChE. However, the calculated total reactivity index (HOMO−LUMO difference) of both HI-6 and K-203 is similar (Table 2), suggesting an explanation for similar binding affinity for GA-inhibited AChE.

The K-oximes have different linker carbon atoms between the two pyridinium moieties and also differences in binding affinity for GA-inhibited AChE oximes. For K-203 and K-075, the linker is a four carbon atom with a C−C double bond, whereas in K-027, K-074, and K-048, the linkers are three and four carbon saturated chains. Table 1 and the optimized geometry of these compounds (Figure 1) show the structural differences. K-203 and K-075 oximes are similar except that one of the oxime moieties in K-203 has been replaced by a carbamoyl group. Although this difference resulted in marginal changes in distance between the bisquaternary nitrogen atoms, molecular volume, and density, the surface area of K-203 decreased by about 7 $Å^2$, a factor that is likely responsible for improving its efficacy by about 3-fold (Table 1). Although Musilek et al. (*13*) did not report the affinity for the inhibited enzyme for cis or trans configurations of K-203 and K-075 in the binding affinity assay, our calculated geometry minimization and optimization methodology indicate the cis configuration of K-203 to be more stable in both gas and aqueous media than the trans, whereas the trans configuration of K-075 was modeled to be more stable in both gas and aqueous media than the cis (Figure 1). This observation suggests that the cis configuration of K-203 is responsible for 3-fold increase in binding affinity as compared to K-075, although K-075 has two terminal oxime moieties, whereas K-203 has one oxime moiety replaced by a carbamoyl moiety. Furthermore, replacement of the oxime moiety with a carbamoyl group in K-203 increased its hydrophilicity and aqueous stabilization by about 8.0 kcal/mol (Table 2) and reduced its calculated octanol/water partition (log *P*) to −0.29. Thus, the increased hydrophilicity and reduced log *P* of K-203 favored its reactivation efficacy and binding affinity for GA-inhibited AChE oximes. On the other hand, these two properties are known to reduce blood−brain barrier penetration (*35, 36*). Although K-048 has a similar carbamoyl substitution for one of the oxime moieties, the conformational flexibility resulting from the saturated four carbon atom linker is likely responsible for its reduced efficacy. Despite having similar conformational flexibility as K-048, K-027 may be more potent due to the shorter distance between the bisquaternary nitrogen atoms due to its three atom saturated carbon linker chain and the resulting combination of stereoelectronic attributes. Inspection of Tables 1 and 2 indicates that K-027 is better stabilized in an aqueous environment, has a more negative log *P*, a lower molecular volume, a lower surface area, and a lower distance of separation between the bisquaternary nitrogen atoms of the pyridinium moieties (N^+-N^+). Interestingly, decreasing the distance between the bisquaternary nitrogen atoms (N^+-N^+ distance) resulted in a predicted decreased toxicity of K-027 (Table 2, as found from our in silico rat oral LD_{50} evaluations).

The most noticeable difference in electronic profiles between K-203 and the other two comparable reactivators, obidoxime and HI-6, is the MEP values (Table 1). The MEP isosurface of a molecule is a measure of the charge distribution from the point of view of an approaching reagent. The deepest red color indicates the most negative electrostatic potential region and, therefore, the nucleophilic power site of a molecule. In contrast, the deepest blue color indicates the most positive electrostatic potential region or most electrophilic region in a molecule. K-203 has a much lower MEP value than obidoxime and HI-6 (Table 2), and the locations of its most negative potential are different in the MEP profiles (Figure 2S of the Supporting Information) in comparison to obidoxime and HI-6. Although the most nucleophilic site in these oximes is located near the hydroxyl oxygen atom, in K-203, it is located by the carbonyl oxygen atom of the carbamoyl group, resulting in a decrease in the intrinsic nucleophilicity of the oxime moiety and also toxicity. Although HI-6 has a similar carbamoyl group at one end of the molecule, the close proximity of the oxime hydroxyl hydrogen atom and the carbamoyl oxygen atom permits an intramolecular hydrogen bond to form and shift the most nucleophilic site to the hydroxyl oxygen atom of the oxime (Figures 1 and Figure 2S of the Supporting Information).

The HOMO and LUMO orbitals and their corresponding isosurfaces are shown in Figures 3S−6S of the Supporting Information. The most likely sites for electrophilic and nucleophilic attack can be visualized in these isosurfaces. These surfaces locate the positions and magnitudes of the HOMO and LUMO where it is available outside the normal steric volume of a molecule for interaction. In these isosurfaces, the lobes that are attacked are color-coded blue. The location, size, and intensity of the blue patches can be interpreted for intermolecular reactivity and assessment for selectivity (*37*). Examination of the HOMO orbitals and isoorbital surfaces of these oximes (Figures 3S and 4S of the Supporting Information) revealed that nucleophilic attack is only possible through the oxime moieties, which is consistent with the reported mechanism of action of these compounds (*6, 7*). Further examination of the HOMO profiles (Figures 3S and 4S of the Supporting Information) indicated that replacement of the second oxime moiety with a carbamoyl group, as in HI-6, K-203, K-027, and K-048, resulted in large changes in the orbitals. The compounds have their HOMO orbitals localized around only the oxime moiety, while the bis oximes have orbitals near both oxime moieties. However, inspection of LUMO orbitals and isoorbital surfaces (Figures 5S and 6S of the Supporting Information) suggested that a nucleophilic attack from the HOMO of an approaching nucleophile is likely to take place on the accessible aromatic ring surface of the compounds, since the larger LUMO lobes (deeper blue color) are located around these regions of the molecules. Examination of the LUMO orbitals and isoorbitals (Figures 5S and 6S of the Supporting Information) revealed sharply different profiles between HI-6 (localized LUMO over the aromatic ring adjacent to the carbamoyl group) and K-203 (two localized LUMO over the two aromatic rings), despite the compounds having similar binding affinity for GA-inhibited AChE. This suggests a mechanism change for nucleophilic attack between the two compounds. Electron transfer from the receptor site to HI-6 and K-203 is likely to be different. K-048 is the only other oxime in this set of compounds that is found to have a LUMO

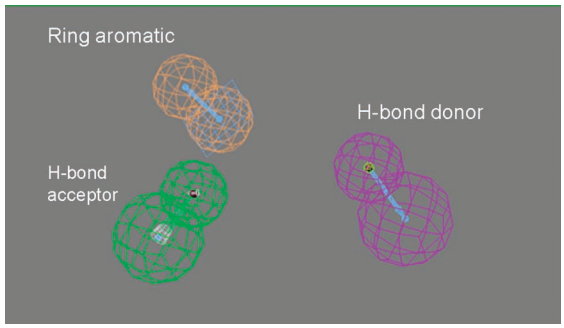

Figure 2. Pharmacophore model for binding affinity of GA-inhibited AChE oximes.

localized by the carbamoyl group, although its optimized geometry is completely different from HI-6 (Figure 1 and Figures 5S and 6S of the Supporting Information). To summarize the results from the above stereoelectronic calculations, the distance between the bisquarternary nitrogen atoms of the two pyridinium rings in the oximes, an optimum hydrophilicity, large surface area, weak electrostatic potential over one of the aromatic rings, low nucleophilicity of the oxime oxygen, and specific locations of the molecular orbitals on the isosurfaces are the stereoelectronic attributes for high potency and reduced toxicity of reactivators for GA-inhibited AChE.

Pharmacophore Model for AChE Affinity for GA Intoxication. We developed a 3D pharmacophore model for binding affinity toward GA-inhibited AChE of the oximes (Chart 1) using the CATALYST methodology (*27*). The model was found to contain one hydrogen bond acceptor function, one hydrogen bond donor function, and one aromatic hydrophobic (aromatic ring) function located in specific geometric regions surrounding the molecular space (Figure 2). The model was generated from the training set of the 11 AChE reactivator oximes (Chart 1) reported by Musilek et al. (*13*) and Kassa et al. (*14*). The binding affinity for the inhibited enzyme expressed as a dissociation constant of the inhibited enzyme−oxime complex of the 11 reactivators was used in the training set and covered a broad range of activity, spanning a K_R of 3.0−2510.0 μM (Table 1). The efficacy of an oxime to reactivate AChE depends on its affinity for the nerve agent-inhibited enzyme, the parameter K_R labeled "affinity for inhibited enzyme" in Table 2 (*13*, *14*). The pharmacophore developed in this paper reflects the affinity of an oxime for the nerve agent-inhibited enzyme, which depends on a variety of physical features that have been modeled (see the Materials and Methods). These features include electrostatic effects, hydrophobic interactions (or more specifically aromatic hydrophobic or aliphatic hydrophobic interactions), hydrogen bond donors, hydrogen bond acceptors, hydrogen bond acceptors (lipid), ionizable sites, and ring aromatic sites. K_R also takes into account the shape, size, surface area, volume, and functional groups of the oxime. This is an important parameter for overall reactivating efficacy because reactivation is related to binding of the oxime to the inhibited enzyme followed by breakdown of the inhibited complex (rate constant of reactivation) (*12*). The series of oximes evaluated here focused on the nerve agent GA. An extreme example of the importance of affinity for inhibited enzyme would be the case where an oxime, such as obidoxime (compound **3**, ref *13*), has high affinity (small K_R) and reactivation efficacy for GA-inhibited enzyme but poor (large K_R) for cyclosarin-inhibited enzyme (*38*). Although the oxime nucleophilicity remains essentially unchanged, obidoxime is a poor reactivator of cyclosarin because it cannot bind to the inhibited enzyme, presumably because the active site with inhibitor precludes appropriate penetration and interaction. Taken together, the pharmacophore developed here describes the general requirements and features of an oxime (or compound with appropriate features) to bind to GA-inhibited enzyme, rather than dissection of the pseudo-first order rate constant of reactivation by the nucleophilic attack of the oxime.

CATALYST methodology (*27*) was used to develop the model by placing suitable constraints on the number of available chemical features, such as aromatic hydrophobic or aliphatic hydrophobic interactions, hydrogen bond donors, hydrogen bond acceptors, lipid hydrogen bond acceptors, and ring aromatic sites, to describe the affinity for the inhibited enzyme of the compounds. The above-discussed results of quantum chemical calculations and the stereoelectronic properties of these compounds provided guidance for calculation of these physicochemical features. The calculated stereoelectronic features, particularly the MEP profiles at the van der Waals surface and at different distances from this surface, can provide an accurate estimate of electron densities in the surrounding space of a molecule, which in turn can guide one in the selection of the features for performing the pharmacophore generation in the CATALYST. For example, a large electron density region in the surrounding space of a molecule would indicate a hydrogen bond acceptor characteristic of a particular atom in the region; similarly, the most positive potential region in a molecule would indicate a hydrogen bond donor atom, and very weak electrostatic potential regions would indicate hydrophobic regions. Although the calculated RHF/6-31G** optimized geometry and its stereoelectronic properties provided the basic guidelines for generation of the pharmacophore, it is important to note that energy minimization of a small molecule alone does not automatically stop at a local minimum of the potential energy surface if the minimum is shallow, thus leading to folding of the molecule and consequently hampering the generation of the bound conformation of a guest in the absence of its host (*39*). Thus, to address this possibility, during the pharmacophore development, molecules were mapped to the features with their predetermined conformations generated using the "fast fit" algorithm in the CATALYST that is technically similar to the reported normal-model-analysis-monitored energy minimization procedure for generating bound conformation (*40*). The conformational energy for developing the set of 3D conformers ranges between 0 to 20 kcal/mol. However, because HI-6 is reported to be highly mobile in the active site of AChE (*8b*) and because its calculated optimized RHF/6-31G** geometry of folded conformation with intramolecular hydrogen bonding may not reflect the derived pharmacophore model, we performed conformation generation using the HI-6 bound conformation taken from crystal structure (*6*) to CATALYST and used the "fast" mode to develop the model (*27*). The procedure resulted in the generation of 10 alternative pharmacophores for affinity of the inhibited enzyme of this training set. The correlation coefficients ranged from 0.93 to 0.87 for 6 of the 10 models, while the remaining four models were found to have below 0.8 correlation coefficients. The total costs of the pharmacophores varied over a narrow range (45−51.5 bits), and the difference between the fixed cost and the null cost was 71 bits, satisfying the acceptable range as recommended in the cost analysis (see the *.log file in the Supporting Information) of the CATALYST procedure (*27*). Notably, the best pharmacophore characterized by one hydrogen bond acceptor function, one hydrogen bond donor function, and one aromatic hydrophobic (aromatic ring) function (Figure 2) is also statistically the most relevant pharmacophore. The predicted affinity for the inhibited enzyme values along with the experimentally determined K_R (μM) values

Table 3. Predicted Binding Affinity Values for GA-Inhibited AChE−Reactivator Complexes along with the Experimentally Determined K_R (μM) Kinetic Values of the Oximes

compound	experimental kinetic parameter, dissociation (K_R) (μM) (*13*, *14*)	predicted kinetic parameter, dissociation (K_R) (μM)	error[a]
obidoxime	3.0	1.8	−1.6
K-203	6.0	13.0	2.2
HI-6	6.0	15.0	2.4
K-075	19.0	26.0	1.4
K-074	29.0	24.0	−1.2
K-027	54.0	62.0	1.1
K-048	93.0	35.0	−2.7
trimedoxime	460.0	200.0	−2.4
2-PAM	575.0	690.0	1.2
K-005	2510.0	1000.0	−2.5
K-033	5.0	11.0	2.3

[a] Values in the error column represent the ratio of estimated activity to experimental activity or its negative inverse if the ratio is less than one. Uncertainty = 3.0.

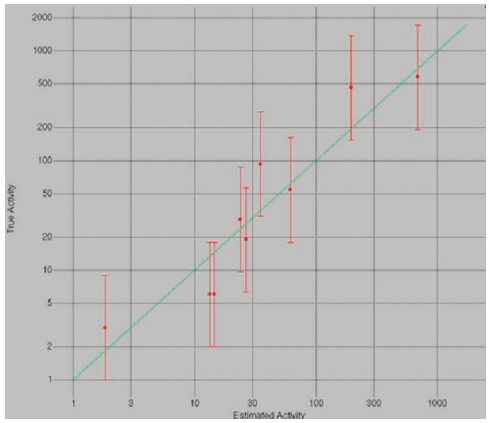

Figure 3. Correlation between experimental and predicted dissociation constants (K_R) (in μM) of the nine GA-inhibited AChE oximes (R = 0.93).

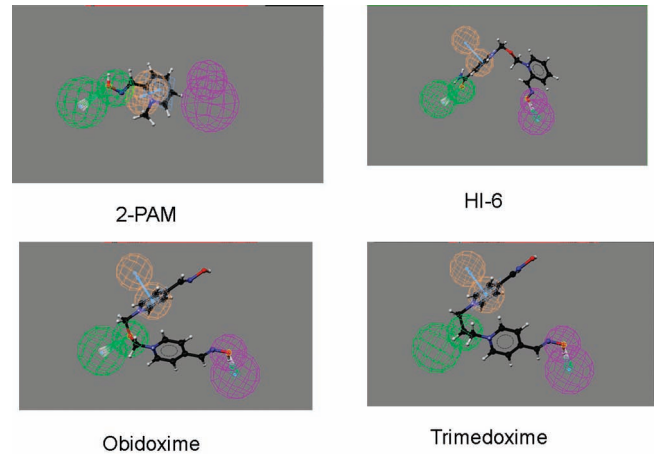

Figure 4. Mapping of the pharmacophore on 2-PAM, HI-6, obidoxime, and trimedoxime showing that the potent analogs map all of the functional features, while the less potent compounds map fewer of the features.

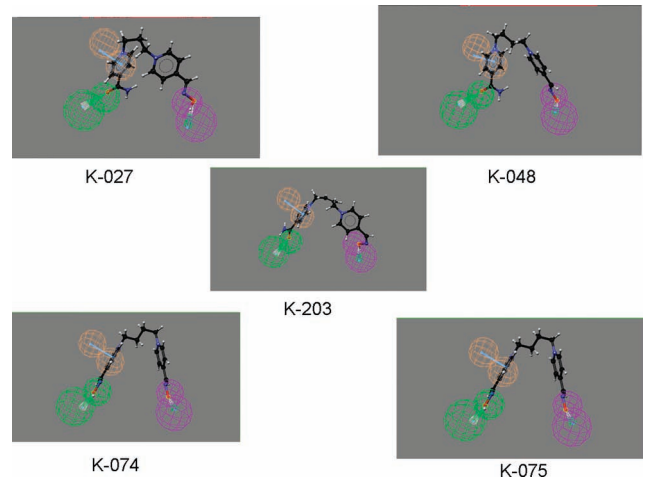

Figure 5. Mapping of the pharmacophore on selected K-oximes showing the potent analogs of the series map all of the functional features, while the less potent compounds map fewer of the features.

of the oximes are presented in Table 3. A plot of experimentally determined K_R (μM) values in the training set and their predicted K_R (μM) values demonstrated an excellent correlation (R = 0.93) within the range of uncertainty 3, indicating the predictive power of the pharmacophore (Figure 3). The statistical significance of the reported pharmacophores (hypotheses) is observed to be well within the recommended range (*27*) of values of the CATALYST procedure. The difference of 70 bits between the fixed and the null cost clearly indicates the robustness of the correlation. Moreover, as the cost difference between the first to the tenth hypothesis and the null hypothesis varies between 66 and 60 bits, it could be expected that for all of these hypotheses, there is about a 90% chance of representing a true correlation (R = 0.9) in the data. Next, the pharmacophore is used to estimate the activities of the oximes in the training set (Table 3). The potent analogs of the series map all of the functional features of the best hypothesis with high scores, for example, obidoxime, HI-6, K-203, K-027, K-048, K-074, and K-075, while the less potent compounds map fewer of the features, for example, 2-PAM and trimedoxime (Figures 4 and 5). Note that the mapping of the pharmacophore onto HI-6 (Figure 4), the folded conformation in the RHF/6-31G** optimized geometry of HI-6, is not seen here, but rather, a conformer similar to the bound conformation in the crystal structure (HI-6 bound GA-inhibited AChE) is observed (*6*). Although HI-6 is not as good a reactivator for GA-inhibited AChE, it binds well to the GA-inhibited AChE. However, its reactivation potency is in the same order of magnitude as obidoxime and more efficacious than trimedoxime. Thus, our pharmacophore model can provide an overall view for an oxime that binds well to the GA-inhibited AChE and differentiates those that do not.

Analysis of the reported X-ray crystal structures of mouse AChE (mAChE) bound with HI-6 and obidoxime (*6*) also shows the importance of the ring aromatic, hydrogen bond acceptor, and hydrogen bond donor features associated with this pharmacophore model. The crystallographic observations are found to support our pharmacophore model. It is commonly believed that despite the possibility of different intermolecular interactions at the peripheral site of the binding pocket of mAChE, the pyridinium ring of the oxime reactivators interacts with the catalytic site in a similar fashion (*8a*). The main feature of the HI-6-bound mAChE crystal structure was the strong cation−π interaction between the 4-carboxylamide-pyridinium ring and the side chains of Tyr124 and Trp 286 (*6*). HI-6 mapped onto the ring aromatic feature of our pharmacophore model (Figure 4) incorporates a cation−π interaction. The carboxylamide moiety of HI-6 is reported to form a hydrogen bond with the main chain Ser298 and water molecule. The hydrogen bond

acceptor feature of our pharmacophore model (Figure 9) accounts for this interaction with HI-6. In addition, it was reported (*6*) that the 2-hydroxy-iminomethylpyridinium ring of HI-6 moves toward the catalytic site interacting with the side chains of Tyr337, Phe338, and Tyr341 via nonbonded contacts and hydrogen bonds. This crystallographic observation also supports the hydrogen bond donor feature of the hydroxyl moiety of the 2-hydroxy-iminomethylpyridinium ring in HI-6 mapped onto the pharmacophore model (Figure 4). Taken together, the above observations of HI-6 bound to the mAChE crystal structure were found to be consistent with our pharmacophore model (Figure 4).

The reported crystal structure of the obidoxime complex with mAChE (*6*) showed that the pyridinium oxime forms a hydrogen bond with the carbonyl oxygen of Val282 and cation$-\pi$ interactions with the side chains of Trp286 and Tyr72. Obidoxime mapped onto the pharmacophore model (Figure 4) was consistent with the X-ray data since the hydrogen bond donor feature supports the formation of a hydrogen bond with the carbonyl oxygen of Val282. Also, the ring aromatic feature of the model should be capable of cation$-\pi$ interactions with the side chains of Trp286 and Tyr72. However, the mapping of hydrogen bond acceptor feature on the ether oxygen atom at the central chain of obidoxime in the pharmacophore model could not be rationalized with the crystal structure where the central chain of obidoxime is accommodated in the active site gorge with no hydrogen-bonding partner for the ether oxygen (*6*).

A recently reported crystallographic study of K-027 bound to mAChE showed that the oxime group of K-027 binds in a similar manner to HI-6 at the Phe295 (*8b*). The carboxyaminopyridinium ring of K-027 is sandwiched by Tyr124 and Trp286, and the 4-oxime pyridinium ring enters the catalytic site parallel to Tyr337 with its oxime oxygen forming hydrogen bonds to the main chain oxygen of His447 and water molecules. Our pharmacophore model mapped onto K-027 (Figure 5) suggests this possibility of K-027 to the hydrogen bond with the main chain oxygen of His447, and it is also observed to be better stabilized in an aqueous environment as seen from its stereoelectronic attributes (Table 2). In summary, although our pharmacophore model was developed solely from SARs of 11 oxime reactivators for GA-inhibited AChE, crystallographic observations support the model (*6, 8a, 8b*).

However, to further reduce chance correlation of the pharmacophore model, in addition to above-discussed statistical analyses, we performed a Fischer randomization as implemented in the CatScramble module of the CATALYST (*27*). This allowed the generation of 19 random spreadsheets from the training set. The statistical significance of the models was calculated. Sixteen of the randomized generated models required a total cost value lower than the model under investigation, indicating an approximately 85% confidence level of our pharmacophore model.

Furthermore, from an additional published report listing dissociation constants, K_R (*28*), of three new K-oximes (none were considered for the training set) and HI-6 evaluated for GA-inhibited AChE, we created a test set and predicted the K_R values of these compounds (Table 4) by conformational mappings of the compounds onto the pharmacophore. The pharmacophore mapped well onto these four compounds (Figure 6). The mappings predicted the K_R values, which are found to be well within the experimental uncertainty. The average error between the experimental and the predicted K_R values is found to be 2.1 for the training set (Table 3) oximes, whereas it is 2.7 for the test set oximes (Table 4); both are within the limit of uncertainty, 3.0, and HI-6 appears to be better predicted in the test set oximes. Thus, the pharmacophore model developed in this study provides predictive value.

Table 4. Experimental and Predicted Binding Affinity (K_R) Values for Four Reported Compounds against GA-Inhibited AChE Reactivation by Mapping the Pharmacophore Model

compound	experimental dissociation (K_R) (μM) (*28*)	predicted dissociation (K_R) (μM)	error[a]
HI-6	27	15	−1.8
1	209	48	−4.3
2	N/A	28	
3	47	120	2.5
4	41	17	2.4

[a] Values in the error column represent the ratio of estimated activity to experimental activity or its negative inverse if the ratio is less than one. Uncertainty = 3.0.

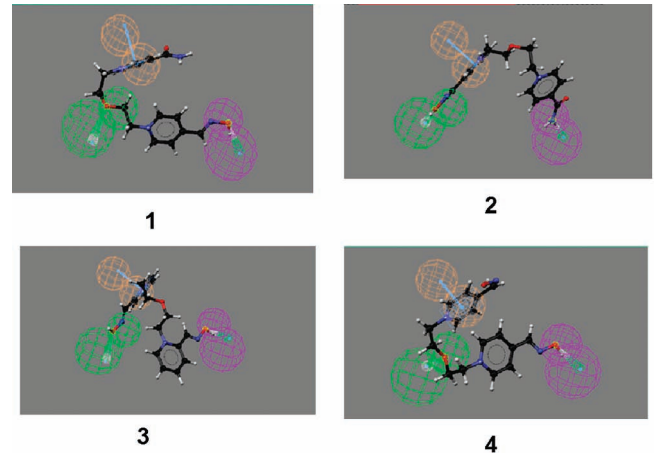

Figure 6. Mapping of the pharmacophore on four test set K-oximes from Table 4 showing the ability of the pharmacophore to predict binding affinity of these compounds against GA-inhibited AChE−reactivator complexes.

Conclusion

Our theoretical study of stereoelectronic properties and generation of an in silico pharmacophore model based on the reactivators of GA-inhibited AChE provided insights on the mechanism of AChE binding affinity for the oximes. Notably, bis-oximes that contain an ether linker between the pyridinium rings increased affinity toward the inhibited AChE and increased the reactivation efficacy as well (*9*). However, the K-oximes contain different linkers, including both saturated and unsaturated carbon chains, which improved oxime efficacy probably due to specific stereoelectronic characteristics. For example, in K-203, the distance between the bisquaternary nitrogen atoms (N^+-N^+), increased hydrophilicity, lower surface area, lower nucleophilic power of the oxime oxygen, and specific location of the predominant HOMO and LUMO orbitals in the isosurfaces together provide the necessary stereoelectronic attributes that enable K-203 to be a better and less toxic reactivator for GA-inhibited AChE.

The in silico pharmacophore model developed here accounted for mouse AChE affinity for HI-6, obidoxime, and K-027 oxime for GA-inhibited AChE. Although our model was developed solely from SARs, it is highly consistent with X-ray crystal structures of AChE with bound reactivators, and the predicted affinity for inhibited enzyme of less toxic oximes from our pharmacophore model was robust (Table 3).

Acknowledgment. Material has been reviewed by the Walter Reed Army Institute of Research. There is no objection to its presentation and/or publication. The opinions or assertions contained herein are the private views of the authors and are not to be construed as official or reflecting true views of the Department of the Army or the Department of Defense. We express sincere thanks to Sonia Thangavelu for drawing the figures and Dr. Shahza Somerville for help in the manuscript preparation. Funding from DTRA (#1E0057_08_WR_C) is gratefully acknowledged.

Supporting Information Available: Statistical significance of the reported pharmacophore, and figures of the following: MEP isodensity surface (RHF/6-31G**), HOMO profiles, HOMO isodensity surfaces, LUMO profiles, and LUMO isodensity surfaces of nine oximes. This material is available free of charge via the Internet at http://pubs.acs.org.

References

(1) Marrs, T. C. (1993) Organophosphate poisoning. *Pharmacol. Ther. 58*, 51–66.
(2) Bakshi, K. S., Pang, S. N. J., and Snyder, R. (2000) Review of the US Army's health risk assessment for oral exposure to six chemical-warfare agents - Introduction to the special issue. *J. Toxicol. Environ. Health A 59*, 282–283.
(3) Sussaman, J. L., Harel, M., Frolow, F., Oefner, C., Goldman, A., Toker, L., and Silman, I. (1991) Atomic structure of acetylcholinesterase from torpedo californica: A prototypic acetylcholine-binding protein. *Science 253*, 872–879.
(4) Barak, D., Kronman, C., Ordentlich, A., Ariel, N., Bromberg, A., Marcus, D., Lazar, A., Velan, B., and Shafferman, A. (1994) Acetylcholinesterase peripheral anionic site degeneracy conferred by amino acid arrays sharing a common core. *J. Biol. Chem. 269*, 6296–6305.
(5) Ekstrom, F., Akfur, C., Tunemalm, A. K., and Lundberg, S. (2006) Structural changes of phenylalanine 338 and histidine 447 revealed by the crystal structures of tabun inhibited murine acetylcholinesterase. *Biochemistry 45*, 74–81.
(6) Ekstrom, F., Pang, Y. P., Boman, M., Artursson, E., Akfur, C., and Borjegren, S. (2006) Crystal structures of acetylcholinesterase in complex with HI-6, ortho-7 and obidoxime: Structural basis for differences in the ability to reactivate tabun conjugates. *Biochem. Pharmacol. 72*, 597–607.
(7) Bajgar, J. (2004) Organophosphates/nerve agent poisoning: mechanism of action, diagnosis, prophylaxis, and treatment. *Adv. Clin. Chem. 38*, 151–216.
(8) (a) Ekstrom, F. J., Astot, C., and Pang, Y. P. (2007) Novel nerve-agent antidote design based on crystallographic and mass spectrometric analyses of tabun-conjugated acetylcholinesterase in complex with antidotes. *Clin. Pharmacol. Ther. 82*, 282–293. (b) Ekstrom, F. J., Hornberg, A., Artursson, E., Hammarstrom, L. G., Schneider, G., and Pang, Y. P. (2009) Structure of HI-6. Sarin-Acetylcholinesterase determined by x-ray crystallography and molecular dynamics simulation: Reactivator mechanism and design. *PLoS ONE 4*, e5957.
(9) Kassa, J., Kuca, K., and Cabal, J. (2005) A comparison of the potency of trimedoxime and other currently available oximes to reactivate tabun-inhibited acetylcholinesterase and eliminate acute toxic effects of tabun. *Biomed. Pap. 149* (2), 419–423.
(10) Musilek, K., Kuca, K., Jun, D., and Dolezal, M. (2007) Progress in synthesis of new acetylcholinesterase reactivators during the period 1990−2004. *Curr. Org. Chem. 11* (2), 229–238.
(11) Jokanovic, M., and Stojiljkovic, M. P. (2006) Current understanding of the application of pyridinium oximes as cholinesterase reactivators in treatment of organophophate posoning. *Eur. J. Pharmacol. 553*, 10–17.
(12) Kuca, K., Cabal, J., Kassa, J., Jun, D., and Hrabinova, M. (2005) A comparison of the potency of the oxime HLö-7 and currently used oximes (HI-6, pralidoxime, obidoxime) to reactivate nerve agent-inhibited rat brain acetylcholinesterase by in vitro methods. *Acta Med. (Hradec Kralove) 48* (2), 81–86.
(13) Musilek, K., Jun, D., Cabal, J., Kassa, J., Gunn-Moore, F., and Kuca, K. (2007) Design of a potent reactivator of tabun-inhibited acetylcholinesterase−Synthesis and evaluation of (*E*)-1-(4-carbamoylpyridinium)-4-(4-hydroxyiminomethylpyridinium)-but-2-ene dibromide (K203). *J. Med. Chem. 50* (22), 5514–5518.
(14) Kassa, J., Kuca, K., Bartosova, L., and Kunesova, G. (2007) The development of new structural analogues of oximes for the antidotal treatment of poisoning by nerve agents and the comparison of their reactivating and therapeutic efficacy with currently available oximes. *Curr. Org. Chem. 11*, 267–283.
(15) Karelson, M., Lobanov, V. S., and Katritzky, A. R. (1996) Quantum-chemical descriptors in QSAR/QSPR studies. *Chem. Rev. 96*, 1027–1044, and references cited therein.
(16) Tomasi, J., Alagona, G., Bonaccorsi, R., Ghio, C., and Canni, R. (1991) *Theoretical Models of Chemical Bonding* (Maksic, Z., Eds.) Part 4, Springer, Berlin.
(17) Murray, J. S., Zilles, B. A., Jayasuriya, K., and Politzer, P. (1986) Comparative analysis of the electrostatic potentials of dibenzofuran and some dibenzo-*p*-dioxins. *J. Am. Chem. Soc. 108*, 915–918.
(18) Gund, P. (2000) Evolution of the pharmacophore concept in pharmaceutical research. In *Pharmacophore Perception, Development and Use in Drug Design* (Güner, O. F., Ed.) pp 5−11, International University Line, La Jolla, CA.
(19) Bhattacharjee, A. K., Geyer, J. A., Woodard, C. L., Kathcart, A. K., Nichols, D. A., Prigge, S. T., Li, Z., Mott, B. T., and Waters, N. C. (2004) A three dimensional in silico pharmacophore model for inhibition of *Plasmodium falciparum* cyclin dependent kinases and discovery of different classes of novel pfmrk specific inhibitors. *J. Med. Chem. 47*, 5418–5426.
(20) Bhattacharjee, A. K. (2007) Virtual screening of compound libraries using *in silico* three dimensional pharmacophores to aid the discovery and design of antimalarial and antileishmanial agents. *Front. Drug Des. Discovery 3*, 257–292.
(21) SPARTAN version 5.1, Wavefunction, Inc., 18401 Von Karman Ave., #370, Irvine, CA 92715.
(22) Dewar, M. J. S., Zoebisch, E. G., Horsley, E. F., and Stewart, J. J. P. (1985) A new general purpose quantum mechanical molecular model. *J. Am. Chem. Soc. 107*, 3902–3909.
(23) Frisch, M. J., Trucks, G. W., Schlegel, H. B., Scuseria, G. E., Robb, M. A., Cheeseman, J. R., Zakrzewski, V. G., Montgomery, J. A., Stratmann, R. E., Burant, S., Dapprich, J. C., Millam, J. M., Daniels, A. D., Kudin, K. N., Strain, M. C., Farkas, O., Tomasi, J., Barone, V., Cossi, M., Cammi, R., Mennucci, B., Pomelli, C., Adamo, C., Clifford, S., Ochterski, J., Petersson, G. A., Ayala, P. Y., Cui, Q., Morokuma, K., Malick, D. K., Rabuck, A. D., Raghavachari, K., Foresman, J. B., Cioslowski, J., Ortiz, J. V., Stefanov, B. B., Liu, G., Liashenko, A., Piskorz, P., Komaromi, I., Gomperts, R., Martin, R. L., Fox, D. J., Keith, T., Al-Laham, M. A., Peng, C. Y., Nanayakkara, A., Gonzalez, C., Challacombe, M., Gill, P. M. W., Johnson, B. G., Chen, W., Wong, M. W., Andres, J. L., Head-Gordon, M., Replogle, E. S., and Pople, J. A. (1998) *Gaussian 98*, Revision A.1, Gaussian, Inc., Pittsburgh, PA.
(24) Mecozzi, S., West, A. P., and Dougherty, D. A. (1996) Cation-pi interactions in simple aromatics: electrostatic provide a predictive model. *J. Am. Chem. Soc. 118*, 2307–2308.
(25) Dixon, R. W., Leonard, J. M., and Hehre, W. J. A. (1993) Continuum solvation model for the AM1 semi-empirical method. *Israel J. Chem. 33*, 427–434.
(26) Tomasi, J., Cammi, R., and Mennucci, B. (1999) Medium effects on the properties of chemical systems: An overview of recent reformulations in the polarizable continuum model (PCM). *Int. J. Quantum Chem. 75*, 767.
(27) CATALYST version 4.10, Accelrys Inc., San Diego, CA.
(28) Kuca, K., Jun, D., Kim, T. H., Cabal, J., and Jung, Y. S. (2006) In vitro evaluation of new acetylcholinesterase reactivators as casual antidotes against tabun and cyclosarin. *Bull. Korean Chem. Soc. 27*, 395–398.
(29) Greenidge, P. A., and Weiser, J. (2001) A comparison of methods for pharmacophore generation with the catalyst software and their use for 3D-QSAR: Application to a set of 4-aminopyridine thrombin inhibitors. *Mini Rev. Med. Chem. 1*, 79–87.
(30) Kuca, K., Jun, D., and Musilek, K. (2006) Structural requirements of acetylcholinesterase reactivators. *Mini Rev. Med. Chem. 6* (3), 269–277.
(31) Kassa, J., Karasova, J., Musilek, K., and Kuca, K. (2008) An evaluation of therapeutic and reactivating effects of newly developed oximes (K156, K203) and commonly used oximes (obidoxime, trimedoxime, HI-6) in tabun-poisoned rats and mice. *Toxicology 243*, 311–316.
(32) Bartosova, L., Kuca, K., Kunesova, G., and Jun, D. (2006) The acute toxicity of acetylcholinesterase reactivators in mice in relation to their structure. *Neurotoxic. Res. 9* (4), 291–296.
(33) TOPKAT 6.1, Accelrys Inc., San Diego, CA.
(34) Lundy, P. M., Raveh, L., and Amitai, G. (2006) Development of the bisquaternary oxime HI-6 toward clinical use in the treatment of organophosphate nerve agent poisoning. *Toxicol. Rev. 25*, 231–43.
(35) Kassa, J., Kuca, K., and Cabal, J. (2005) A comparison of the efficacy of currently available oximes against tabun in rats. *Biologia 60* (17), 77–79.

(36) Bajgar, J., Fusek, J., Kuca, K., Bartosova, L., and Jun, D. (2007) Treatment of organophosphate intoxication using cholinesterase reactivators: facts and fiction. *Mini Rev. Med. Chem. 7* (5), 461–466.
(37) Bhattacharjee, A. K., and Karle, J. M. (1999) Stereoelectronic properties of antimalarial artemisinin analogues in relation to neurotoxicity. *Chem. Res. Toxicol. 12*, 422–428.
(38) Kuca, K., Patočka, J., Cabal, J., and Jun, J. (2004) Reactivation of organophosphate-inhibited acetylcholinesterase by quaternary pyridinium aldoximes. *Neurotoxic. Res. 6* (7−8), 565–570.
(39) Wang, Q., and Pang, Y. P. (2007) Normal-mode-analysis-monitored energy minimization procedure for generating small-molecule bound conformations. *PLoS 2* (10), e1025.
(40) Wang, Q., and Pang, Y. P. (2007) Preference of small molecules for local minimum conformations when binding to proteins. *PLoS 2* (9), e820.

TX900192U